$\Lambda(1405)$ and $\bar{\Lambda}(1405)$ in J/ψ four-body decays

Chiangbing Li and E. Oset
Departamento de Física Teórica and IFIC, Centro Mixto Universidad de Valencia–CSIC, Institutos de Investigación de Paterna, Apdo. Correos 22085, 46071 Valencia, Spain
(Received 23 April 2004; published 13 December 2004)

We study the structure of the baryon resonances $\Lambda(1405)$ and $\bar{\Lambda}(1405)$ in J/ψ four-body decays $J/\psi \to \Sigma\bar{\Sigma}\pi\pi$ in the framework of a coupled channel chiral unitary approach. With still sufficient freedom for model parameters, the $\Lambda(1405)$ and $\bar{\Lambda}(1405)$ resonances are generated by simultaneously taking the meson baryon and meson antibaryon final state interactions into account. The $\pi\Sigma$ ($\pi\bar{\Sigma}$) invariant mass distributions peak around 1410 MeV, which favors the assertion that the $\Lambda(1405)$ [$\bar{\Lambda}(1405)$] is a superposition of the two $\Lambda(1405)$ [$\bar{\Lambda}(1405)$] states which dominantly couple to $\bar{K}N$ ($K\bar{N}$) and $\pi\Sigma$ ($\pi\bar{\Sigma}$), respectively. We also calculate the amplitude for isospin $I=1$ which gives hints of a possible $I=1$ baryon resonance in the energy region of the $\Lambda(1405)$, which up to now has not been observed.

DOI: 10.1103/PhysRevC.70.065202 PACS number(s): 13.75.Lb, 12.39.Fe

I. INTRODUCTION

The case of the $\Lambda(1405)$ is one of the examples of dynamically generated resonances which was already described within scattering theory with coupled channels in [1]. More recently the advent of nonperturbative methods with input from the chiral Lagrangian has set that original idea on firmer grounds [2–9]. The $\Lambda(1405)$ resonance, appearing about 30 MeV below the $\bar{K}N$ threshold, plays a key role in the $\bar{K}N$ interaction and related processes and is a subject of debate concerning its nature, whether it is a genuine three-quark system [10,11] or a molecularlike meson-baryon bound state where chiral dynamics plays an important role. The recent discovery of the pentaquark [12] should stimulate again the debate on the nature of the $\Lambda(1405)$ since the existence of that exotic state forces an interpretation of that baryon with at least five quarks [13,14], although molecular structures with $K\pi N$ (heptaquark) have also been investigated [15,16]. Within the chiral approach of [2–9] the $\Lambda(1405)$ stands as a quasibound state of the meson-baryon, mostly $\bar{K}N$ and $\pi\Sigma$, which is also equivalent to five quarks in the quark picture. The existence of the pentaquark makes more easily acceptable the idea of other *pentaquark* nonexotic states, and vice versa. No doubt, explorations on the nature of the $\Lambda(1405)$ will provide more clues to understand the nonperturbative nature of the QCD dynamics.

Chiral perturbation theory (ChPT) directly deals with hadron interactions in terms of meson-baryon degrees of freedom. As an effective field theory which incorporates the chiral symmetry of QCD, ChPT has proved to be very successful in describing hadron interactions at low energies by expanding the chiral Lagrangian in powers of the hadron momentum. However, due to the problem of convergence of ChPT at relatively higher energies where most meson and baryon resonances appear, the plain ChPT can do little for the description of resonances. The lowest energy resonance in $\pi\pi$ scattering is the σ which appears as a pole in the complex plane with a very large width. This is the case in the chiral unitary approach discussed below [17,18] and is also the case in the $\pi\pi$ scattering amplitudes constructed by the Roy equation in [19], where the width is as big as the real part of $\sim$500 MeV. Although this pole, far away from the real axis, has small repercussion at low energies where perturbative chiral calculations can be correctly applied, the existence of the complex variable theorem stating that a series expansion has a radius of convergence till the first singularity already sets the limits on how far the perturbation expansion can be pushed.

The chiral unitary coupled channels approach, which makes use of the standard ChPT Lagrangian together with an implicit or explicit expansion of $\mathrm{Re}T^{-1}$, instead of the T matrix, has proved to be very successful in describing meson-meson [17,18] and meson-baryon [6] interactions at higher energies. By employing the chiral Lagrangian at the lowest order and solving the Bethe-Salpeter equation, this method was able to reproduce well the low lying meson and baryon resonances in the Particle Data Group (PDG) [17,18,20]. When doing the extrapolation of ChPT at higher energies one usually neglects crossing symmetry since only the right hand cut is used as a source of the imaginary part of the amplitude and the left hand cut (unphysical cut) is neglected. This, however, can be improved, as was done in [21] for the meson-meson interaction. Also in [4] a systematic method is proposed to also account for the left hand cut by including perturbative crossed loop diagrams in the kernel of a dispersion relation for T^{-1}. In [21] it was found that the effect of the left hand cut was very small in a wide range of energies for the meson-meson interaction below $\sqrt{s}=1.2$ GeV. Similarly, in [4] the effect of the left hand cut was estimated to be even smaller since crossed terms are reduced by factors of $(q/2M)^2$ (with M the baryon mass) in the meson-baryon interaction, which are very small at the energies where the low lying baryon resonances appear. The accuracy of the approximation neglecting the left hand cut has an important technical advantage since, as proved in [4], the dispersion relation requires only the imaginary part of the meson-baryon loop (on shell part) and this leads to a Bethe-Salpeter

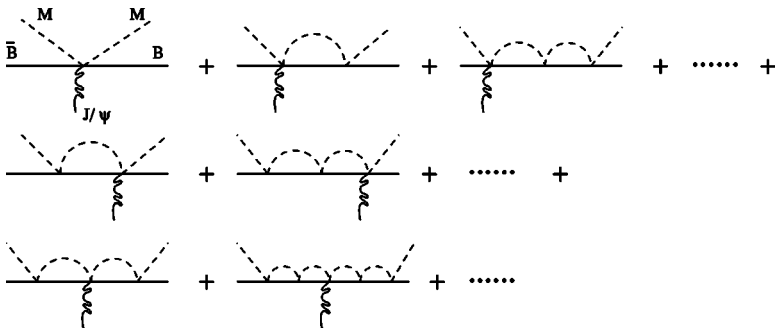

FIG. 1. Diagrams for $J/\psi \to B\bar{B}MM$ decays including the meson-baryon and meson-antibaryon final state interactions.

(BS) type equation, identical to the one used in [6,17], where the kernel (potential) is needed only on shell. This converts the BS equation into an algebraic equation, much as it happens with the use of a separable interaction, although there is no need to define such a separable kernel.

With this chiral unitary approach the authors of [22] calculated the photoproduction of the $\Lambda(1405)$ on the proton and nuclei and found different shapes of $\pi\Sigma$ invariant mass distributions in different $\pi\Sigma$ charge channels, which was lately experimentally confirmed in [23] and gave support to the assumption that the $\Lambda(1405)$ is a meson-baryon loosely bound state. Additionally, it was found in [24] that the SU(3) symmetry breaking leads to two poles of the $\bar{K}N$ scattering matrix that might be responsible for the nominal $\Lambda(1405)$, one dominantly coupling to $\pi\Sigma$ and the other to $\bar{K}N$, and these poles are the mixing of the SU(3) singlet and octet. It was concluded there that there are two $\Lambda(1405)$ resonances and the experimentally observed one is a superposition of the two states. However, whether the two poles really exist in the $\Lambda(1405)$ region is still unsolved experimentally. For this aim the authors of Ref. [25] suggested isolating the pole of $\Lambda(1405)$ that couples dominantly to $\bar{K}N$ in a photoinduced K^* vector meson production process. It will be interesting to further study the structure of $\Lambda(1405)$ in particular processes.

In this work we propose to extract the structure of the $\Lambda(1405)$ in the decay processes $J/\psi \to \Sigma\bar{\Sigma}\pi\pi$ using the coupled channel chiral unitary approach to account for meson-baryon and meson-antibaryon final state interactions (FSI). It is worth noting that in these processes the $\bar{\Lambda}(1405)$ could be generated through the $M\bar{B}$ FSI, together with the $\Lambda(1405)$ generated through the MB FSI, and this would provide valuable information on the structure of the resonances. The J/ψ four-body decays have been proposed to provide further information on the low lying meson resonances in Ref. [26], where the chiral unitary approach was employed to account for meson-meson FSI without considering the MB FSI. A natural continuation of the work of [26] is to look for the meson-baryon FSI that can lead to the formation of resonances, particularly those which in the chiral unitary approach are dynamically generated. Experimental interest in the issue has been shown in a recent effort to search for the pentaquark state in J/ψ four-body decays $J/\psi \to K_S^0 p K^- \bar{n}$ and $J/\psi \to K_S^0 \bar{p} K^+ n$ [27].

II. THE MODEL

We proceed now to construct the amplitudes for $J/\psi \to B\bar{B}MM$ simultaneously taking MB and $M\bar{B}$ FSI into account, which is diagrammatically described in Fig. 1.

Due to the lack of knowledge on the dynamics of charmonium decays, we employ the phenomenological Lagrangian used in [26] which incorporates SU(3) symmetry to account for the vertex of J/ψ four-body decays. Assuming that the J/ψ is an SU(3) singlet [28], the most general $BBMM$ Lagrangians of SU(3) scalar nature without derivatives in the fields have the following possible structures:

$$\mathcal{L}_1 = g\,\mathrm{Tr}[\bar{B}\gamma^\mu B\Phi\Phi]\Psi_\mu, \quad \mathcal{L}_2 = g\,\mathrm{Tr}[\bar{B}\gamma^\mu \Phi B\Phi]\Psi_\mu,$$

$$\mathcal{L}_3 = g\,\mathrm{Tr}[\bar{B}\gamma^\mu \Phi\Phi B]\Psi_\mu, \quad \mathcal{L}_4 = g\,\mathrm{Tr}[\bar{B}\gamma^\mu B]\mathrm{Tr}[\Phi\Phi]\Psi_\mu, \tag{1}$$

with Φ, B the ordinary SU(3) matrices for pseudoscalar mesons and $\frac{1}{2}^+$ baryons, respectively, Ψ_μ the J/Ψ field, and g a constant to provide the right dimensions. In constructing the effective Lagrangians we have imposed SU(3) symmetry to the Lagrangians together with the requirement of a minimum number of derivatives in the fields. We deliberately do not search for Lagrangians implementing chiral symmetry, which in view of the large number of particles involved and the fact that derivatives in the field are implied, would blow up the number of possible structures. Chiral Lagrangians are particularly useful to show how the interaction would change in the chiral limit when quark masses go to zero, but if the purpose is to have a parametrization of an amplitude accounting for the possible SU(3) structures, a procedure like the one done here is sufficient within a limited range of energies. This is more the case in an approach like ours, in which, as noted above, a factorization of on shell vertices is implicit in the loop, which will not cause derivative couplings to bring extra divergences. Similar effective Lagrangians, without derivatives in the fields, have been used in related problems of J/ψ decay, like $J/\psi \to \phi\pi\pi$ [29,30]. As discussed in [29], the use of other Lagrangians involving derivatives of the fields does not change the results and conclusions.

We then take the Lagrangian of our problem as a linear combination of $\mathcal{L}_a$, $a=1,2,\ldots,4$,

$$\mathcal{L} = \sum_{a=1}^{4} x_a \mathcal{L}_a. \tag{2}$$

This leads to the vertex for $J/\psi \to (M\bar{B})_i (MB)_j$

TABLE I. $\tilde{c}_{ij}$ coefficients for $J/\psi \to (M\overline{B})_i(MB)_j$ decays.

	K^-p	$\overline{K^0}n$	$\pi^0\Lambda$	$\pi^0\Sigma^0$	$\eta\Lambda$	$\eta\Sigma^0$	$\pi^+\Sigma^-$	$\pi^-\Sigma^+$
$K^+\overline{p}$	x_1+ x_3+2x_4	x_3	$\frac{x_1}{2\sqrt{3}}+$ $\frac{x_2}{2\sqrt{3}}-\frac{x_3}{\sqrt{3}}$	$\frac{x_1}{2}+\frac{x_2}{2}$	$-\frac{x_1}{6}+$ $\frac{5x_2}{6}+\frac{x_3}{3}$	$-\frac{x_1}{2\sqrt{3}}+$ $\frac{x_2}{2\sqrt{3}}$	x_2	x_1
$K^0\overline{n}$		x_1+ x_3+2x_4	$-\frac{x_1}{2\sqrt{3}}-$ $\frac{x_2}{2\sqrt{3}}+\frac{x_3}{\sqrt{3}}$	$\frac{x_1}{2}+\frac{x_2}{2}$	$-\frac{x_1}{6}+$ $\frac{5x_2}{6}+\frac{x_3}{3}$	$\frac{x_1}{2\sqrt{3}}-$ $\frac{x_2}{2\sqrt{3}}$	x_1	x_2
$\pi^0\overline{\Lambda}$			$\frac{x_1}{3}+\frac{x_2}{3}+$ $\frac{x_3}{3}+2x_4$	0	0	$\frac{x_1}{3}+\frac{x_2}{3}+$ $\frac{x_3}{3}$	0	0
$\pi^0\overline{\Sigma^0}$				x_1+x_2+ x_3+2x_4	$\frac{x_1}{3}+\frac{x_2}{3}+$ $\frac{x_3}{3}$	0	x_2	x_2
$\eta\overline{\Lambda}$					x_1+x_2+ x_3+2x_4	0	$\frac{x_1}{3}+$ $\frac{x_2}{3}+\frac{x_3}{3}$	$\frac{x_1}{3}+$ $\frac{x_2}{3}+\frac{x_3}{3}$
$\eta\overline{\Sigma^0}$						$\frac{x_1}{3}+\frac{x_2}{3}+$ $\frac{x_3}{3}+2x_4$	$-\frac{x_1}{\sqrt{3}}+$ $\frac{x_3}{\sqrt{3}}$	$\frac{x_1}{\sqrt{3}}-\frac{x_3}{\sqrt{3}}$
$\pi^-\overline{\Sigma^-}$							x_1+ x_3+2x_4	x_2
$\pi^+\overline{\Sigma^+}$								x_1+ x_3+2x_4

$$\tilde{V}_{ij} = -\tilde{c}_{ij} g \overline{u_j}(p') \gamma^\mu v_i(p) \epsilon_\mu(J/\psi), \tag{3}$$

where we have already specified that we have a baryon-antibaryon production, rather than the baryon destruction and creation that one has for the meson-baryon amplitude. The eight coupled $(MB)_i$ ($i=1, 2, \ldots, 8$) channels that we consider are K^-p, $\overline{K^0}n$, $\pi^0\Lambda$, $\pi^0\Sigma^0$, $\eta\Lambda$, $\eta\Sigma^0$, $\pi^+\Sigma^-$, and $\pi^-\Sigma^+$, and the $(M\overline{B})_i$ channels are $K^+\overline{p}$, $K^0\overline{n}$, $\pi^0\overline{\Lambda}$, $\pi^0\overline{\Sigma^0}$, $\eta\overline{\Lambda}$, $\eta\overline{\Sigma^0}$, $\pi^-\overline{\Sigma^-}$, and $\pi^+\overline{\Sigma^+}$. The $K\Xi$ state was shown in [6] to have no relevance in the $\Lambda(1405)$ dynamics. We list the $\tilde{c}_{ij}$ coefficients in Table I and we note that $\tilde{c}_{ji}=\tilde{c}_{ij}$.

In the rest frame of J/ψ, $\epsilon_r^0(J/\psi)=0$ for the three polarization vectors and Eq. (3) in the nonrelativistic approximation for the nucleons can be written as

$$\tilde{V}_{ij} = \tilde{c}_{ij} g \vec{\sigma} \cdot \vec{\epsilon}(J/\psi) \tag{4}$$

with $\vec{\sigma}$ the standard Pauli matrices.

We then construct the $J/\psi \to (M\overline{B})_i(MB)_j$ amplitudes involving both MB and $M\overline{B}$ FSI. The decay amplitude with only MB FSI can be written as

$$T_{ij} = \tilde{V}_{ij} + \sum_k \tilde{V}_{ik} G_k t_{kj}, \tag{5}$$

where t_{kj} are the scattering amplitudes for $(MB)_k \to (MB)_j$ which have been calculated in Ref. [6]. The $(MB)_k$ loop integrals

$$G_k = i \int \frac{d^4q}{(2\pi)^4} \frac{M_k}{E_k(\vec{q})} \frac{1}{k^0 + p^0 - q^0 - E_k(\vec{q}) + i\epsilon} \frac{1}{q^2 - m_k^2 + i\epsilon}$$
$$= \int \frac{d^3q}{(2\pi)^3} \frac{1}{2\omega_k(q)} \frac{M_k}{E_k(\vec{q})} \frac{1}{p^0 + k^0 - \omega_k(\vec{q}) - E_k(\vec{q}) + i\epsilon} \tag{6}$$

depend only on the MB invariant mass $p^0 + k^0 = \sqrt{s}$, where p and k are the momentum of the final baryon and meson, respectively, the masses of the particles, and the cutoff of the meson three-momentum in the loop $q_{\max}$. In Eq. (6) M_k and E_k are the mass and energy of the baryon in the loop, respectively, and $\omega_k = \sqrt{\vec{q}^2 + m_k^2}$ is the energy of the meson with the mass m_k in the loop. The amplitudes T_{ij} in Eq. (5) are functions of $\sqrt{s}$ once $q_{\max}$ is fixed. In our calculation we take $q_{\max} = 630$ MeV. The value of $q_{\max}$ was fixed in [6] in order to get an agreement of the theory with the lower energy parameters of the $K^- p$ interaction, and with only this parameter the $K^- p$ scattering cross sections and the invariant mass distribution of the $\Lambda(1405)$ resonance were well reproduced. Proper behavior of the loop functions requires that this cutoff be reasonably bigger than the on shell momenta of the particles inside the loops. This puts some limit to the range of energies where this can be used. A dimensional regularization of the loops was done in [4,20] but the two procedures are practically equivalent as shown in [4] by establishing a correspondence between the cutoff and the subtraction constant in dimensional regularization. In [20] it was found that the cutoff method could be safely used up to energies of $\sqrt{s} = 1670$ MeV where the $\Lambda(1670)$ resonance is dynamically generated.

The final amplitudes for J/ψ four-body decays taking both MB and $M\bar{B}$ FSI into account can be constructed as

$$\tilde{T}_{ij} = T_{ij} + \sum_k \bar{t}_{ik} \bar{G}_k T_{kj} = \tilde{V}_{ij} + \sum_k \tilde{V}_{ik} G_k t_{kj} + \sum_k \bar{t}_{ik} \bar{G}_k \tilde{V}_{kj}$$
$$+ \sum_{kl} \bar{t}_{ik} \bar{G}_k \tilde{V}_{kl} G_l t_{lj}, \tag{7}$$

where $\bar{t}_{ik}$ are the scattering amplitudes for $(M\bar{B})_i \to (M\bar{B})_k$ and $\bar{G}_k$ is the $(M\bar{B})_k$ loop integration as given in Eq. (6). It can be seen that Eq. (7) exactly corresponds to the diagrammatic description in Fig. 1. Taking the same value as the $q_{\max}$ of the G loop integration for the cutoff in the $\bar{G}$ loop integration, the $\bar{t}$ and $\bar{G}$ matrices are identical to the t and G matrices derived in Ref. [6], respectively, although they are functions of the $M\bar{B}$ invariant masses $\sqrt{s'}$. Hence the amplitudes $\tilde{T}_{ij}$ in Eq. (7) are functions of $\sqrt{s}$ and $\sqrt{s'}$.

In Eqs. (5) and (7), the MB and $M\bar{B}$ amplitudes in the loops are taken on shell. It was shown in [6] that the contribution of the off shell parts could be reabsorbed into a redefinition of coupling constants in MB scattering. Analogously, for the loop involving the vertex $\tilde{V}_{ij}$ in Eq. (5), which has a different structure from the one involving the MB amplitude, the contribution of the off shell part in the loop could be absorbed by renormalizing the coupling constant g in Eq. (1) since the integration for the off shell part in just one loop has the same structure as the tree diagram [6]. Similar arguments also apply for the off shell part of $M\bar{B}$ loops in Eq. (7).

In this paper we do not consider the $M\bar{M}$ interaction nor the $B\bar{B}$ interaction. The neglect of the $B\bar{B}$ interaction is justified since we are taking the phenomenological Lagrangians of Eq. (1) which were used in [26] and fitted to the experimental data without taking into account the $B\bar{B}$ interaction. Then the effect of $B\bar{B}$ interaction in the region of energies of interest is accounted for phenomenologically in the couplings fitted to experiment in [26]. This is, however, not the case for the MM interaction since this one was taken into account explicitly in [26]. However, the choice of different regions of phase space in [26] and the present work justifies the neglect of the MB interaction in [26] and of the MM interaction in the present work. The basic point is that the meson-meson interaction is relatively weak except in the region of the resonances. These would be in the case of meson-meson interaction the $f_0(980)$ and $a_0(980)$ and to a much smaller extent the broad σ, κ of the $\pi\pi, \pi K$ interaction. In the case of MB interaction, the resonance of relevance in the region studied here is the $\Lambda(1405)$. When we concentrate in a narrow region around 1405 MeV for the invariant mass of $\pi\Sigma$ and in addition in the same region of energies for the invariant mass of the $\pi\bar{\Sigma}$, one selects a very narrow region of the four-body phase space where there is a large enhancement because of the double resonance structure of $\pi\Sigma$ and $\pi\bar{\Sigma}$. However, this region of phase space contains the whole range of invariant masses of the meson-meson combinations, and thus the possible effects of the MM resonances are diluted since the MM resonance region will only appear in a very narrow region of the phase space where one is integrating. A practical manifestation of this disentangling of the interactions when one looks at peaks of resonances in particular channels is seen in [22] where one studies the $\gamma p \to K^+ \pi\Sigma$ with $\pi\Sigma$ in the $\Lambda(1405)$ resonance region. The MB interaction is considered there but the MM interaction is neglected and the predictions show good agreement with experimental results [23]. Conversely, in [31] the same reaction was used, paying attention to the meson-meson interaction alone, in order to evaluate cross sections for the production of scalar mesons.

III. RESULTS AND DISCUSSION

The mass distribution of the decays $J/\psi \to (M\bar{B})_i (MB)_j$ with respect to the MB and $M\bar{B}$ invariant masses, which is particularly suited to search for resonances, can be written as [32]

$$\frac{d^2\Gamma_{ij}}{dM_I dM_I'} = \frac{1}{(2\pi)^8 2M_J} \frac{\pi^3}{2M_J^2 M_I^2 M_I'^2} 4M_I M_I' M M'$$
$$\times \lambda^{1/2}(M_I^2, m^2, M^2) \lambda^{1/2}(M_I'^2, m'^2, M'^2)$$
$$\times \lambda^{1/2}(M_I^2, M_I'^2, M_J^2) \overline{\sum} \sum |\tilde{T}_{ij}(M_I, M_I')|^2, \tag{8}$$

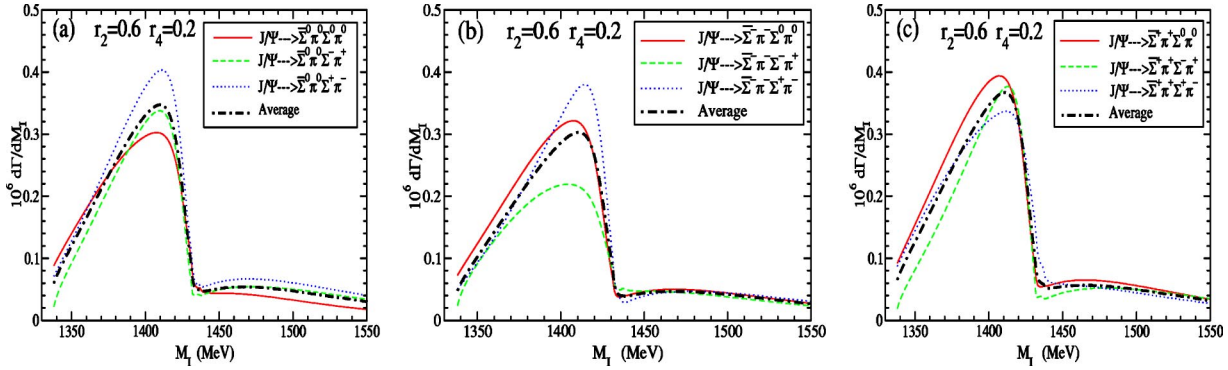

FIG. 2. (Color online) The $\pi\Sigma$ invariant mass distributions to account for $\Lambda(1405)$ for $J/\psi\to\Sigma\bar{\Sigma}\pi\pi$ decays with the model parameters $r_2=0.6$, $r_4=0.2$, where the involved meson and baryons are assigned physical masses.

with M_I and M_I' being the MB and $M\bar{B}$ invariant masses, respectively, m and m' the meson masses in the final states, M and M' the B and $\bar{B}$ masses, respectively, M_J the mass of J/ψ, and $\lambda(x^2,y^2,z^2)$ the Kaellen function. Equation (8) differs slightly from Eq. (46) of [32] because of our different normalization of the fields and the $\tilde{T}$ matrix. It should be stated that the simple form of this equation holds because of our neglect of the meson-meson and baryon-antibaryon interactions. We shall come back to this point at the end of this section.

We then perform calculations for the decays $J/\psi\to\Sigma\bar{\Sigma}\pi\pi$ to search for the $\Lambda(1405)$ and $\bar{\Lambda}(1405)$. We have the x_i with $i=1, 2, \ldots, 4$ in Eq. (2) as the model parameters. Similarly to what was done in [26], we define the ratios $r_i=x_i/x_3$ with $i=1,2,4$, which were evaluated by fitting the experimental data of $J/\psi\to p\bar{p}\pi^+\pi^-$ decay. It was shown in [26] that the parameter r_1 influences the shape of the $\pi\pi$ spectrum of $J/\psi\to p\bar{p}\pi^+\pi^-$ at higher energies, but its contribution could be included in the variation of r_4. The parameter r_2 does not influence the $J/\psi\to p\bar{p}\pi^+\pi^-$ but plays an important role for the decays considered here. In our calculations r_4 is given the values of Ref. [26], which reproduces the empirical $\pi\pi$ spectrum in $J/\psi\to p\bar{p}\pi^+\pi^-$ decay. We take $r_4=0.2$, which has been used in Ref. [26]. As for r_2 we take it as a free parameter and vary it in a wide range from 0.1 to 2.0. Although the branching ratio obtained varies much, the important thing from which the conclusions will be drawn is the shape of the distribution and this does not depend on the precise value of r_2. Similarly, changes in r_2 for the value $r_4=-0.27$, which was also able to well reproduce the data for $J/\psi\to p\bar{p}\pi^+\pi^-$, as is shown in Ref. [26] within a reasonable range, also do not change the qualitative character of the results for the channels considered here. In the following we take $r_4=0.2$ and $r_2=0.6$ to give characteristic descriptions for the generation of $\Lambda(1405)$ and $\bar{\Lambda}(1405)$ in $J/\psi\to\Sigma\bar{\Sigma}\pi\pi$ decays. Then we have the value of the constant $g_\alpha=(x_3+2x_4)g=1.1\times10^{-6}$ MeV^{-2}, which determines the shape of the $\pi\pi$ spectrum and the width of the decay $J/\psi\to p\bar{p}\pi^+\pi^-$ [26].

We present the $\pi\Sigma$ invariant mass distributions for the nine $J/\psi\to\Sigma\bar{\Sigma}\pi\pi$ decay channels in Fig. 2, where baryons and mesons are assigned physical masses. It can be seen that the shapes of the distributions are quite different from each other, where all coupled channels collaborate to build up the $\Lambda(1405)$ resonance. The figure has labels like $J/\psi\to\bar{\Sigma}^-\pi^-\Sigma^0\pi^0$, etc., which means that one measures simultaneously the $\bar{\Sigma}^-\pi^-$ and $\Sigma^0\pi^0$ and integrates Eq. (8) over the invariant mass of $\bar{\Sigma}^-\pi^-$ to provide the $\Sigma^0\pi^0$ mass distribution shown in the figure. Similarly, we could plot the figure for $d\Gamma/dM_I'$ for the invariant mass of the $\bar{\Sigma}^-\pi^-$ and other channels integrating over the invariant mass of the $\pi\Sigma$ system. Certainly channels like $J/\psi\to\bar{\Sigma}^-\pi^-\Sigma^-\pi^+$ would have identical distributions for the $\bar{\Sigma}^-\pi^-$ or $\Sigma^-\pi^+$ invariant masses. For other combinations one finds small differences between $\bar{\Sigma}\pi$ and $\Sigma\pi$ mass distributions because of small mass differences of the involved Σ baryons and π mesons.

The results in Fig. 2 can be better understood with the isospin decomposition for $\pi\Sigma$,

$$|\pi^0\Sigma^0\rangle=\sqrt{\frac{2}{3}}|2,0\rangle-\sqrt{\frac{1}{3}}|0,0\rangle,$$

$$|\pi^+\Sigma^-\rangle=-\sqrt{\frac{1}{6}}|2,0\rangle-\sqrt{\frac{1}{2}}|1,0\rangle-\sqrt{\frac{1}{3}}|0,0\rangle,$$

$$|\pi^-\Sigma^+\rangle=-\sqrt{\frac{1}{6}}|2,0\rangle+\sqrt{\frac{1}{2}}|1,0\rangle-\sqrt{\frac{1}{3}}|0,0\rangle, \qquad (9)$$

and for $\pi\bar{\Sigma}$

$$|\pi^0\bar{\Sigma}^0\rangle=\sqrt{\frac{2}{3}}|2,0\rangle-\sqrt{\frac{1}{3}}|0,0\rangle,$$

$$|\pi^-\bar{\Sigma}^-\rangle=-\sqrt{\frac{1}{6}}|2,0\rangle+\sqrt{\frac{1}{2}}|1,0\rangle-\sqrt{\frac{1}{3}}|0,0\rangle,$$

$$|\pi^+\bar{\Sigma}^+\rangle=-\sqrt{\frac{1}{6}}|2,0\rangle-\sqrt{\frac{1}{2}}|1,0\rangle-\sqrt{\frac{1}{3}}|0,0\rangle. \qquad (10)$$

With $|\pi^+\rangle=-|1,1\rangle$, $|\Sigma^+\rangle=-|1,1\rangle$, and $|\bar{\Sigma}^-\rangle=-|1,1\rangle$, we have the amplitudes for the particular $J/\psi\to(M\bar{B})_i(MB)_j$ decays:

$$\tilde{T}_{44}=\frac{2}{3}T^{(2)}+\frac{1}{3}T^{(0)},$$

$$\tilde{T}_{47} = -\frac{1}{3}T^{(2)} + \frac{1}{3}T^{(0)},$$

$$\tilde{T}_{48} = -\frac{1}{3}T^{(2)} + \frac{1}{3}T^{(0)},$$

$$\tilde{T}_{77} = \frac{1}{6}T^{(2)} - \frac{1}{2}T^{(1)} + \frac{1}{3}T^{(0)},$$

$$\tilde{T}_{78} = \frac{1}{6}T^{(2)} + \frac{1}{2}T^{(1)} + \frac{1}{3}T^{(0)},$$

$$\tilde{T}_{88} = \frac{1}{6}T^{(2)} - \frac{1}{2}T^{(1)} + \frac{1}{3}T^{(0)}, \quad (11)$$

and we note $\tilde{T}_{ij} = \tilde{T}_{ji}$. It can be seen that the shapes for the particular decay channels show evidence of some isospin breaking which appears naturally in our framework because of the different masses of the members of the same isospin multiplet. This is the case, for instance, of the channels $J/\psi \to \bar{\Sigma}^0 \pi^0 \Sigma^- \pi^+$ and $J/\psi \to \bar{\Sigma}^0 \pi^0 \Sigma^+ \pi^-$ (channels 47 and 48) in Fig. 2(a), which according to Eq. (11) should give the same distributions. Similarly, the distributions of the channels $J/\psi \to \bar{\Sigma}^- \pi^- \Sigma^0 \pi^0$ in Fig. 2(b) and $J/\psi \to \bar{\Sigma}^+ \pi^+ \Sigma^0 \pi^0$ in Fig. 2(c) (channels 74 and 84, respectively) should also be equal. The larger differences that one observes in Fig. 2(b) between $J/\psi \to \bar{\Sigma}^- \pi^- \Sigma^- \pi^+$ and $J/\psi \to \bar{\Sigma}^- \pi^- \Sigma^+ \pi^-$ (channels 77 and 78, respectively) are due to mixed terms of the type $\mathrm{Re}(T^{(1)}T^{(2)*})$ and $\mathrm{Re}(T^{(1)}T^{(0)*})$, implying, in this case, that these terms are larger than the differences due to isospin breaking.

In Fig. 2 we have also calculated the averaged cross sections. By using again Eqs. (11) it is easy to see that all the mixed terms $\mathrm{Re}(T^{(i)}T^{(j)*})$ in the modulus squared of the amplitudes cancel in these averages and one has only contributions of $|T^{(i)}|^2$. These averages should not be the same since they come from different combinations of $|T^{(i)}|^2$, but the fact that they are not very different indicates that they are all dominated by the $|T^{(0)}|^2$ component, which appears in all of them with the same weight, $\frac{1}{3}|T^{(0)}|^2$, and that the other isospin components are much smaller. Hence, this averaged distribution is the closest thing one can get experimentally for the shape of the $\Lambda(1405)$ resonance. From the position of the peak of the distribution around 1410 MeV and the width of around 60 MeV, the results imply that we have a superposition of the two $\Lambda(1405)$ $[\bar{\Lambda}(1405)]$ resonances [with poles at $(1390 - i60)$ MeV and $(1426 - i16)$ MeV] found in [24].

Now we turn to another interesting potential use of these reactions. It was found in [4] that there was a pole of $I=1$ close to the $\bar{K}N$ threshold which would correspond to a new resonance not accounted for in the Particle Data Book. Under certain circumstances, with smaller degree of SU(3) breaking, it was also found in [24] using the approach of [20]. It is interesting to see what these reactions can say in this respect. For instance, from Eq. (11) we see

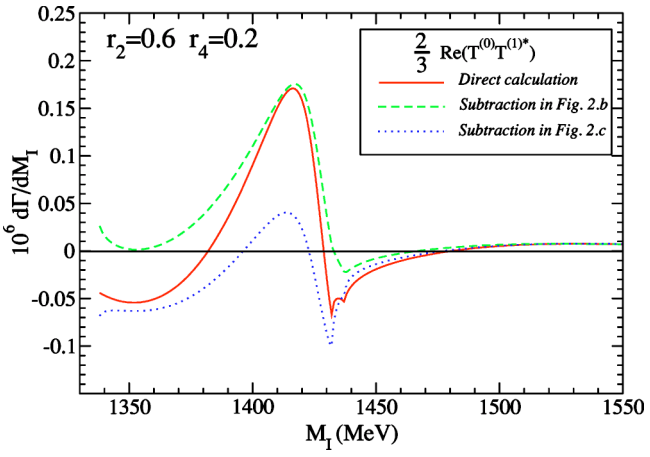

FIG. 3. (Color online) The $\pi\bar{\Sigma}$ invariant mass distribution for the $(2/3)\mathrm{Re}(T^{(0)}T^{(1)*})$ of $J/\psi \to \Sigma\bar{\Sigma}\pi\pi$. The solid line denotes the results through direct theoretical calculations and the dashed and dotted lines are the results calculated by subtracting the $\pi\bar{\Sigma}$ invariant mass distributions of the particular decays $J/\psi \to \bar{\Sigma}^- \pi^- \Sigma^- \pi^+$ and $J/\psi \to \bar{\Sigma}^- \pi^- \Sigma^+ \pi^-$ in Fig. 2(b) and $J/\psi \to \bar{\Sigma}^+ \pi^+ \Sigma^- \pi^+$ and $J/\psi \to \bar{\Sigma}^+ \pi^+ \Sigma^+ \pi^-$ in Fig. 2(c), respectively.

$$|\tilde{T}_{78}|^2 - |\tilde{T}_{77}|^2 = |\tilde{T}_{87}|^2 - |\tilde{T}_{88}|^2 = \frac{2}{3}\mathrm{Re}(T^{(0)}T^{(1)*}) + \frac{1}{3}\mathrm{Re}(T^{(1)}T^{(2)*}), \quad (12)$$

where the $T^{(1)}T^{(2)*}$ term is negligible. This means that the subtraction of the mass distributions of the charged decay channels $J/\psi \to \bar{\Sigma}^- \pi^- \Sigma^+ \pi^-$ and $J/\psi \to \bar{\Sigma}^- \pi^- \Sigma^- \pi^+$ can give hints on the $T^{(1)}$ amplitude, given that the amplitude $T^{(0)}$ can in principle be derived by averaging the mass distributions for particular $J/\psi \to \bar{\Sigma}\pi\Sigma\pi$ decays. In Fig. 3 we plot two different results. One is done by calculating $T^{(0)}$ and $T^{(1)}$ from combinations of the amplitudes given in Eqs. (11). Then a mass distribution is generated by replacing $\bar{\Sigma}\Sigma|\tilde{T}|^2$ in Eq. (8) with $\frac{2}{3}\mathrm{Re}(T^{(0)}T^{(1)*})$. The second calculation corresponds to what an experimentalist could do by subtracting the two mass distributions corresponding to the $J/\psi \to \bar{\Sigma}^- \pi^- \Sigma^+ \pi^-$ and $J/\psi \to \bar{\Sigma}^- \pi^- \Sigma^- \pi^+$ channels in Fig. 2(b) or $J/\psi \to \bar{\Sigma}^+ \pi^+ \Sigma^+ \pi^-$ and $J/\psi \to \bar{\Sigma}^+ \pi^+ \Sigma^- \pi^+$ channels in Fig. 2(c). The considerably different magnitude between the results of the two subtractions in Fig. 3 is the manifestation of the isospin symmetry breaking that we have in this approach. With isospin symmetry the two subtractions give approximately the same results. The $T^{(1)}$ amplitude could in principle be extracted from Fig. 3 and compared to the theoretically calculated one. For this purpose, in Fig. 4 we show the real part and imaginary parts of $T^{(1)}$ directly calculated in our model for some fixed values of the $M\bar{B}$ invariant masses. It can be seen that the shape of the $T^{(1)}$ does not qualitatively change with respect to the selected values of M_I' and there exist nontrivial cusps around the energy $M_I = 1420$ MeV, which may give some hints for the possible approximate resonant structure predicted in [4,24]. Calling attention to the fact that the reactions discussed here bear potentially valu-

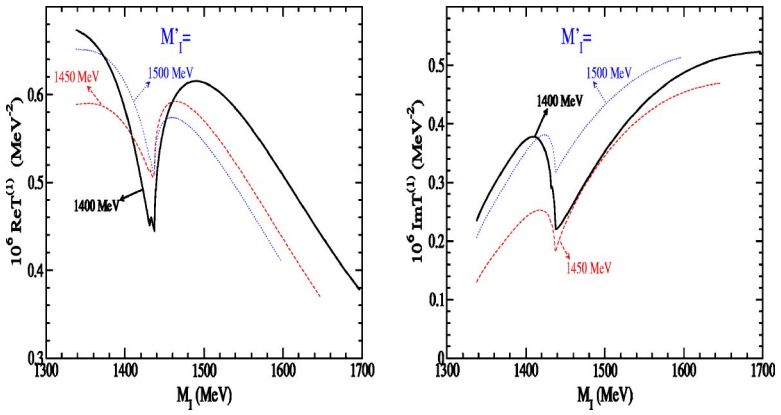

FIG. 4. (Color online) The real part and imaginary part of the $T^{(1)}$ amplitude as a function of M_I for different values of the $\pi\overline{\Sigma}$ invariant masses.

able information about this $I=1$ amplitude is one of the purposes of the present work.

The calculations have been done using the cutoff of $q_{\max}=630$ MeV used in [6]. This cutoff was the only free parameter there to fit different $\overline{K}N$ cross sections, threshold values plus the $\Lambda(1405)$ shape. The freedom in this parameter is very small if a good fit to these data is demanded. Changes in the parameter from 630 to 620 or 640 MeV are as much as one can afford. We have reevaluated our results with these new values of the parameter and find changes of about 10% in the cross sections. These should be considered as theoretical uncertainties from this source.

So far we have taken into account the meson-baryon (meson-antibaryon) interaction only. Since in [26], by studying the same problem, we took into account the meson-meson interaction, with some additional work we can consider the two sources of interactions to see how our results can change with the inclusion of the meson-meson interaction. The new calculation has been done by adding to the diagrams of Fig. 1 the rescattering diagrams of Fig. 1 of Ref. [26]. This means we would consider the diagrams with meson rescattering stemming from the first diagram in Fig. 1 of the present paper. The neglect of the rescattering terms from the other diagrams can be justified by the fact that the two pions can be produced at reasonably large distances where this interaction should be very weak. We must now modify Eq. (8) since the $\tilde{T}$ matrix now depends on other variables. The standard formula in this case is

$$d\Gamma = \frac{(2\pi)^4}{2M_J}|\tilde{T}|^2 d\Phi(P;p_1,p_2,k_1,k_2) \tag{13}$$

with the four-body phase space being

$$d\Phi(P;p_1,p_2,k_1,k_2) = \delta^4(P-p_1-p_2-k_1-k_2)\frac{d^3p_1}{(2\pi)^3}\frac{M_1}{E(p_1)} \times \frac{d^3p_2}{(2\pi)^3}\frac{M_2}{E(p_2)}\frac{d^3k_1}{(2\pi)^3} \times \frac{1}{2\omega(k_1)}\frac{d^3k_2}{(2\pi)^3}\frac{1}{2\omega(k_2)}, \tag{14}$$

where P is the four-momentum of J/ψ, p_i and k_i $(i=1,2)$ the four-momenta of the involved baryons and mesons, respectively, M_i the baryon masses, and $E(p_i)=\sqrt{M_i^2+p_i^2}$ and $\omega(k_i)=\sqrt{m_i^2+k_i^2}$, with m_i being meson masses, the baryon and meson energies, respectively. We perform the integrations with the Monte Carlo method. We show the results in Fig. 5 for the channel $J/\psi\to\overline{\Sigma}^0\pi^0\Sigma^0\pi^0$ (results are similar for other channels). We observe that the strength in the region of energies above 1405 MeV gets considerably increased, smearing the meson resonance contribution in a large phase

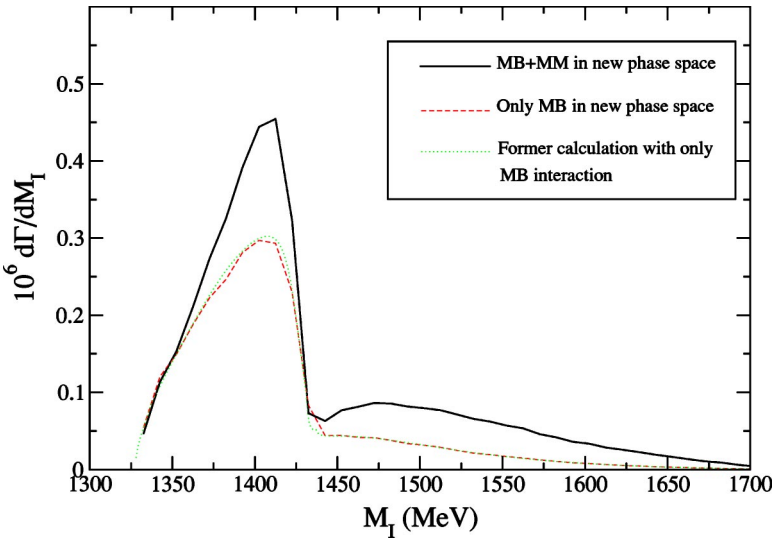

FIG. 5. (Color online) The $\pi\Sigma$ invariant mass distribution of the $J/\psi\to\overline{\Sigma}^0\pi^0\Sigma^0\pi^0$ channel calculated in the new phase space of Eq. (13) with the Monte Carlo method. Solid line, the result in the new phase space considering both meson-baryon and meson-meson interactions; dashed line, the result in the new phase space considering only meson-baryon interactions; dotted line, the result calculated with Eq. (8) considering only meson-baryon interactions.

space region. We also observe that the shape of the $\Lambda(1405)$ peak is not changed but there is an extra strength which accounts for about 30% of the total. This reflects a constructive interference between the resonance amplitude and the background from the meson-meson interaction. This extra contribution coming from the consideration of the meson-meson interaction changes the strength of the peak in about the same amount in the different channels and does not affect the qualitative nature of the conclusions drawn here.

IV. SUMMARY

In summary, we investigated the structure of the baryon resonances $\Lambda(1405)$ and $\bar{\Lambda}(1405)$ in J/ψ four-body decays $J/\psi \to \Sigma\bar{\Sigma}\pi\pi$. It is shown that $\Lambda(1405)$ and $\bar{\Lambda}(1405)$ are generated by simultaneously taking the FSI of $\pi\Sigma$ and $\pi\bar{\Sigma}$ into account, which is calculated in the framework of the chiral unitary approach. By averaging the three $\pi\Sigma$ ($\pi\bar{\Sigma}$) mass distributions in either of the three plots in Fig. 2 we get the real shape for the nominal $\Lambda(1405)$ [$\bar{\Lambda}(1405)$] resonance, which peaks around 1410 MeV and is a superposition of the two $\Lambda(1405)$ states discussed in [24]. On the other hand, the subtraction of the charged decay channels in either Fig. 2(b) or Fig. 2(c) gives hints of the possible $I=1$ resonance in the energy region of $\Lambda(1405)$, which up to now has not been observed. From an experimental point of view, although all the nine particular $J/\psi \to \Sigma\bar{\Sigma}\pi\pi$ decays were considered here for a theoretical analysis, the three of them in either Fig. 2(b) or Fig. 2(c) are practically adequate to extract the structure of $\Lambda(1405)$, $\bar{\Lambda}(1405)$, and the possible $I=1$ resonance in this region. It is worth noting that our theoretical calculations were done with still sufficient freedom of model parameters. However, the fact that the variation of the parameters within a reasonable range does not change the qualitative feature of the results, together with the success of the chiral unitary approach in past work, sets the predictions made here on firmer grounds. Experimental data on these channels would be most welcome to further fix the model parameters and to get refined predictions. No doubt, the experimental investigations on the proposed J/ψ four-body decays will provide interesting information of the structure of $\Lambda(1405)$ and $\bar{\Lambda}(1405)$ resonances and valuable test for the approaches employed here.

ACKNOWLEDGMENTS

We would like to thank M. J. Vicente Vacas for valuable discussions. C.L. acknowledges the hospitality of the University of Valencia where this work has been done and financial support from the Ministerio de Educacion in the program Doctores y Tecnólogos Extranjeros under Contract No. SB2000-0233. This work is partly supported by DG-ICYT Project No. M2003-00856 and the EU network EURIDICE Contract No. HPRN-CT-2002-00311.

[1] M. Jones, R. H. Dalitz, and R. R. Horgan, Nucl. Phys. **B129**, 45 (1977).
[2] N. Kaiser, P. B. Siegel, and W. Weise, Nucl. Phys. **A594**, 325 (1995).
[3] N. Kaiser, T. Waas, and W. Weise, Nucl. Phys. **A612**, 297 (1997).
[4] J. A. Oller and U. G. Meissner, Phys. Lett. B **500**, 263 (2001).
[5] U.-G. Meißner and J. A. Oller, Phys. Rev. D **64**, 014006 (2001).
[6] E. Oset and A. Ramos, Nucl. Phys. **A635**, 99 (1998).
[7] D. Jido, A. Hosaka, J. C. Nacher, E. Oset, and A. Ramos, Phys. Rev. C **66**, 025203 (2002).
[8] C. Garcia-Recio, J. Nieves, E. Ruiz Arriola, and M. J. Vicente Vacas, Phys. Rev. D **67**, 076009 (2003).
[9] C. Garcia-Recio, M. F. M. Lutz, and J. Nieves, Phys. Lett. B **582**, 49 (2004).
[10] N. Isgur and G. Karl, Phys. Rev. D **18**, 4187 (1978).
[11] M. Kimura *et al.*, Phys. Rev. C **62**, 015206 (2000).
[12] LEPS Collaboration, T. Nakano *et al.*, Phys. Rev. Lett. **91**, 012002 (2003).
[13] A. Hosaka, Phys. Lett. B **571**, 55 (2003).
[14] R. L. Jaffe and F. Wilczek, Phys. Rev. Lett. **91**, 232003 (2003).
[15] P. Bicudo and G. M. Marques, Phys. Rev. D **69**, 011503 (2004).
[16] F. Llanes-Estrada, E. Oset, and V. Mateu, Phys. Rev. C **69**, 055203 (2004).
[17] J. A. Oller and E. Oset, Nucl. Phys. **A620**, 438 (1997); **A652**, 407(E) (1999).
[18] J. A. Oller, E. Oset, and J. R. Peláez, Phys. Rev. D **59**, 074001 (1999); **60**, 099906(E) (1999).
[19] G. Colangelo, J. Gasser, and H. Leutwyler, Nucl. Phys. **B603**, 125 (2001).
[20] E. Oset, A. Ramos, and C. Bennhold, Phys. Lett. B **527**, 99 (2002).
[21] J. A. Oller and E. Oset, Phys. Rev. D **60**, 074023 (1999).
[22] J. C. Nacher, E. Oset, H. Toki, and A. Ramos, Phys. Lett. B **455**, 55 (1999).
[23] LEPS Collaboration, J. K. Ahn *et al.*, Nucl. Phys. **A721**, 715 (2003).
[24] D. Jido, J. A. Oller, E. Oset, A. Ramos, and U. G. Meissner, Nucl. Phys. **A725**, 181 (2003).
[25] T. Hyodo, A. Hosaka, M. J. Vicente Vacas, and E. Oset, Phys. Lett. B **593**, 75 (2004).
[26] Chiangbing Li, E. Oset, and M. J. Vicente Vacas, Phys. Rev. C **69**, 015201 (2004).
[27] J. Z. Bai *et al.*, Phys. Rev. D **70**, 012004 (2004).
[28] Fayyazuddin and Riazuddin, *A Modern Introduction of Particle Physics* (World Scientific, Singapore, 1992), p. 275.
[29] Ulf-G. Meissner and J. A. Oller, Nucl. Phys. **A679**, 671 (2001).
[30] L. Roca, J. E. Palomar, E. Oset, and H. C. Chiang, Nucl. Phys. **A744**, 127 (2004).
[31] E. Marco, E. Oset, and H. Toki, Phys. Rev. C **60**, 015202 (1999).
[32] P. Nyborg, H. S. Song, W. Kernan, and R. H. Good, Jr., Phys. Rev. **140**, B914 (1965).